

Tortuous Microvessels Contribute to Wound Healing via Sprouting Angiogenesis

Diana C. Chong, Zhixian Yu, Hailey E. Brighton, James E. Bear, Victoria L. Bautch

Objective—Wound healing is accompanied by neoangiogenesis, and new vessels are thought to originate primarily from the microcirculation; however, how these vessels form and resolve during wound healing is poorly understood. Here, we investigated properties of the smallest capillaries during wound healing to determine their spatial organization and the kinetics of formation and resolution.

Approach and Results—We used intravital imaging and high-resolution microscopy to identify a new type of vessel in wounds, called tortuous microvessels. Longitudinal studies showed that tortuous microvessels increased in frequency after injury, normalized as the wound healed, and were closely associated with the wound site. Tortuous microvessels had aberrant cell shapes, increased permeability, and distinct interactions with circulating microspheres, suggesting altered flow dynamics. Moreover, tortuous microvessels disproportionately contributed to wound angiogenesis by sprouting exuberantly and significantly more frequently than nearby normal capillaries.

Conclusions—A new type of transient wound vessel, tortuous microvessels, sprout dynamically and disproportionately contribute to wound-healing neoangiogenesis, likely as a result of altered properties downstream of flow disturbances. These new findings suggest entry points for therapeutic intervention.



Visual Overview—An online [visual overview](#) is available for this article. (*Arterioscler Thromb Vasc Biol.* 2017;37:1903-1912. DOI: 10.1161/ATVBAHA.117.309993.)

Key Words: angiogenesis ■ cell shape ■ intravital imaging ■ microcirculation ■ tortuous microvessels ■ wound healing

Angiogenesis, the formation of new blood vessels via sprouting, is a complex process whereby endothelial cells migrate out from preexisting vessels and form new connections to increase the vascular network.¹⁻⁵ During development, angiogenesis occurs in response to tissue cues, such as hypoxia, and is critical for proper growth of the embryo.⁵⁻⁷ In contrast, endothelial cells are largely quiescent in adults; however, they become activated to reinstate angiogenesis in physiological processes, such as wound healing, or in diseases, such as cancer.⁸ Unlike developmental angiogenesis, physiological angiogenesis is often characterized by the formation of tortuous vessels.⁹⁻¹² For example, tortuous vessels are associated with wound healing,¹³ placenta formation during pregnancy,¹⁴ and arteriogenesis that often accompanies ischemia.¹⁵ Tortuous vessels have a distinct morphology, displaying S-shaped curves, oscillations, or kinks compared with normal linear vessels, and they are often excessively permeable.¹⁶ Although tortuous vessels have been observed for decades, it is not clear how these vessels form, how they contribute to angiogenesis, or how they resolve.

Wound healing is characterized by several phases,¹⁷⁻¹⁹ including a proliferative phase in which angiogenesis is a major component. Tortuous vessels often appear during the proliferative phase, and their occurrence decreases as the wound heals.¹³ Tortuous vessels are thought to result from increased cytokine and growth factor signaling, changes in flow dynamics, changes in extracellular matrix composition, and decreased mural cell coverage.^{9,16} Tortuous vessels also have increased permeability,²⁰ which may facilitate delivery to the wound site. Tortuous vessels have been examined at the macro level via immunohistochemistry and intravital imaging, corrosion casting, and scanning electron microscopy.^{13,16,21-23} However, it remains unclear whether tortuosity extends to the smallest capillaries that are the source of most wound-healing angiogenesis, and the cellular parameters associated with formation and resolution of vessel tortuosity are poorly understood.

Here, we used intravital imaging to analyze the role of tortuous capillary vessels, called tortuous microvessels, during wound healing. Longitudinal analysis of healing in the mouse ear allowed for capture of vessel dynamics over time. Similar to larger vessels, tortuous microvessel frequency increased and then gradually decreased

See cover image

Received on: March 31, 2017; final version accepted on: August 1, 2017.

From the Curriculum in Genetics and Molecular Biology (D.C.C., Z.Y., V.L.B.), Department of Biology (V.L.B.), Lineberger Comprehensive Cancer Center (J.E.B., V.L.B.), McAllister Heart Institute (V.L.B.), and Department of Cell Biology and Physiology (H.E.B., J.E.B.), The University of North Carolina at Chapel Hill.

The online-only Data Supplement is available with this article at <http://atvb.ahajournals.org/lookup/suppl/doi:10.1161/ATVBAHA.117.309993/-/DC1>.

Correspondence to Victoria L. Bautch, PhD, Department of Biology, CB No. 3280, The University of North Carolina at Chapel Hill, Chapel Hill, NC 27599. E-mail bautch@med.unc.edu

© 2017 The Authors. *Arteriosclerosis, Thrombosis, and Vascular Biology* is published on behalf of the American Heart Association, Inc., by Wolters Kluwer Health, Inc. This is an open access article under the terms of the Creative Commons Attribution Non-Commercial-NoDerivs License, which permits use, distribution, and reproduction in any medium, provided that the original work is properly cited, the use is noncommercial, and no modifications or adaptations are made.

Arterioscler Thromb Vasc Biol is available at <http://atvb.ahajournals.org>

DOI: 10.1161/ATVBAHA.117.309993

Nonstandard Abbreviations and Acronyms	
dpw	days post-wounding

relative to normal capillaries in the wound site. High-resolution imaging in vivo revealed that endothelial cells comprising tortuous microvessels have aberrant cell shapes, increased permeability, and suggest altered flow dynamics. Surprisingly, tortuous microvessels have increased sprouting compared with normal capillaries, indicating for the first time that tortuous vessels contribute to sprouting angiogenesis during wound healing. Thus, we identify a new type of tortuous vessel that forms from the smallest capillaries and contributes significantly to sprouting angiogenesis in wounds. Because of its exuberant sprouting, this class of vessel may be a novel interventional target for improved wound healing.

Materials and Methods

Materials and Methods are available in the [online-only Data Supplement](#).

Results

Tortuous Microvessels Are Associated With Wound Healing

To better understand the role of angiogenesis in wound healing, we investigated this process in a mouse ear wound-healing model. We used a *Fli1*-GFP vascular reporter line²⁴ and a small ear punch biopsy (0.35 mm) to induce a wound, and we examined angiogenesis and tortuous vessel formation as the wound healed. Using intravital imaging and 2-photon microscopy, we acquired high-resolution images (including the Z plane) of small caliber vessels growing into the wound site of the same mouse ear over an extended time period (≤ 39 days post-wounding, dpw; Figure 1A through 1C; Figure IA in the [online-only Data Supplement](#)). Image analysis revealed that small-caliber tortuous vessels, which we termed tortuous microvessels, were present in the wound area as early as 3 dpw, alongside normal small capillaries (Figure 1D through 1I).

We defined a tortuous microvessel as having a diameter of 5 to 20 μm and oscillating S curves, kinks, bends, or twists. To accurately quantify tortuous microvessels during wound healing, we applied a tortuosity index to vessel segments by examining the ratio between total segment length (L_c) and the shortest distance between start and end point (L_e), then multiplying the ratio by the number of times the vessel changed direction or curved $<160^\circ$ (N_c ; Figure 1J through 1L). We found that tortuosity index values for tortuous microvessels were significantly higher than those for normal nearby microvessels in the wound, verifying that this vessel type has a distinct morphology that can be quantified (Figure 1L). Tracing of all microvessels in the images revealed that the total length of microvessels significantly increased from 3 to 17 dpw, coinciding with the angiogenic phase of wound healing, then leveled off during subsequent times (Figure 1B in the [online-only Data Supplement](#)). We then categorized the vessels into normal or tortuous subgroups, which revealed that the percentage of tortuous microvessels also followed this time course initially and peaked at 17 dpw; however, tortuous microvessels then

significantly decreased as healing progressed (Figure 1M). Comparison of start, peak, and end points showed that the percentage increase in tortuous microvessels was significant at 17 dpw compared with the beginning and end of the imaging time (Figure 1N). Thus, tortuous microvessel formation increased initially as part of an overall trend, but then decreased while overall microvessel length stabilized, suggesting that tortuous microvessels resolve into normal capillaries over time.

To more closely examine the relationship between tortuous microvessels and wound closure, we measured microvessel location relative to the wound. Circular regions were outlined every 100 μm outward from the wound center and used to calculate the percentage of tortuous microvessels in these regions at each time point (Figure 2A and 2B) for 31 days. We found that the majority of vessels near the wound boundary (100–300 μm from centroid) were tortuous. Because most tortuous microvessels were found close to the wound boundary, we next asked how tortuous microvessels formed in new tissue that is initially avascular. We outlined the avascular area (including the biopsy punch hole) around the wound at 1 dpw and used this constant area to assess new angiogenesis at subsequent time points (Figure 2C; Figure IIA and IIB in the [online-only Data Supplement](#)). The area remained avascular until 5 dpw, and subsequent vascularization consisted mainly of tortuous microvessels at early time points (7–17 dpw; Figure 2D). However, as the wound remodeled, the total length of the tortuous microvessels decreased, while the total length of the normal capillaries in this area increased, and the 2 lengths were equal by 31 to 39 dpw. To determine whether the predominant vascularization by tortuous microvessels at the early time points was because of angiogenesis, tissue migration into the wound area, or a combination of both, we tracked the location of distinct vessels in this region over time. We found that the wound area initially showed some mass movement, suggesting that microvessels may move in because of larger tissue displacement at early time points (Figure IIB in the [online-only Data Supplement](#)). However, we tracked individual patterns over time and found that starting around 7 to 9 dpw, mass movement was minimal, and new microvessels appeared to form via sprouting angiogenesis into the avascular region (Figure IIB in the [online-only Data Supplement](#)). These findings suggest that sprouting angiogenesis is the driving force behind vascularization of new tissue after a short burst of tissue displacement and that sprouting angiogenesis is active at the wound border where tortuous microvessels are concentrated.

We next hypothesized that the shift from tortuous to normal microvessels in the avascular area resulted at least in part from resolution of tortuous vessels, and we temporally tracked individual tortuous microvessels over time to test this hypothesis (Figure 2E and 2F). We found that 69% of tortuous microvessels normalized, while 27% of microvessels remained tortuous over the time course of wound healing, suggesting that tortuous microvessel formation and resolution is a dynamic process associated with the angiogenic phase of wound healing.

Tortuous Microvessel Endothelial Cells Have Distinct Properties

We took advantage of high-resolution intravital imaging to interrogate the endothelial cells that line tortuous microvessels. The topology of tortuous microvessels suggested that

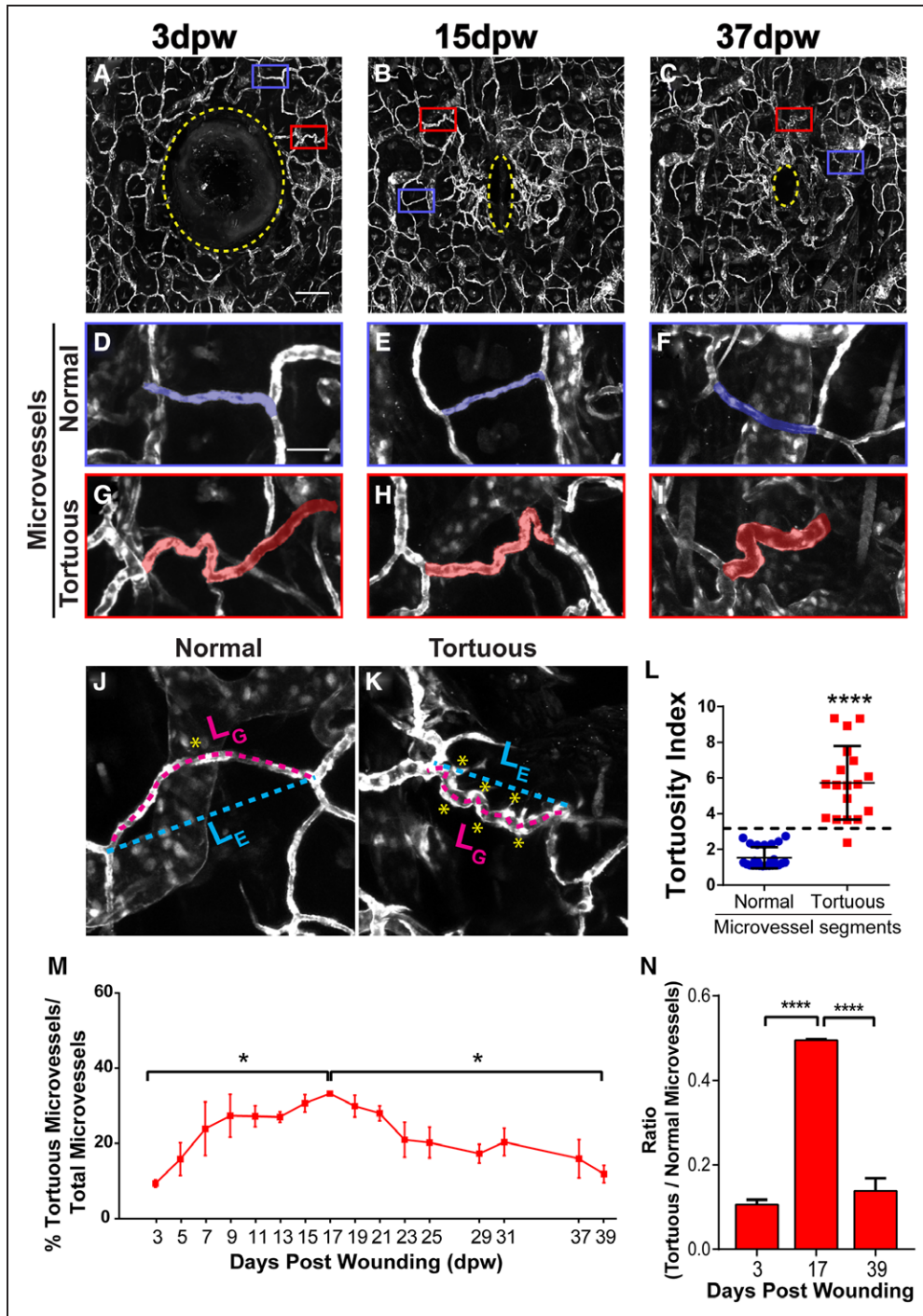


Figure 1. Tortuous microvessels during wound healing. **A–C**, Wound and surrounding vasculature at indicated times. Yellow stippled line, wound punch and avascular area; boxes, areas magnified below. **D–F**, High magnification vasculature of blue boxed areas showing normal microvessels. **G–I**, High magnification of red boxed areas showing tortuous microvessels. **J** and **K**, Examples of normal and tortuous microvessel segments used to calculate tortuosity index. **L**, Quantification of normal and tortuous microvessel segments. **M**, Quantification of percentage of tortuous microvessels over 39 days, $n=3$ ears. **N**, Graph representing the ratio of tortuous to normal microvessels at indicated times, $n=3$ ears. Error bars, mean \pm SEM; Statistical comparisons by 2-way ANOVA with Tukey multiple comparison test; * $P<0.05$; **** $P<0.0005$. Scale bars: 200 μ m (**A**), 50 μ m (**D**). Vessels pseudocolored using Photoshop. ANOVA indicates analysis of variance; and dpw, days post-wounding.

similar to larger tortuous vessels, they experience disturbed flow, and as a result, the endothelial cells may change shape and acquire other properties consistent with changes that promote vessel sprouting, defined as a state of activation.²⁵ We acquired images from live intravital imaging while injecting

small-diameter (100 nm) fluorescent microspheres to visualize blood flow. Before injection, there were no red fluorescent microspheres present in any vessels (Figure 3A; Movie in the [online-only Data Supplement](#)). On injection, the microspheres moved through the imaging field quickly in areas with

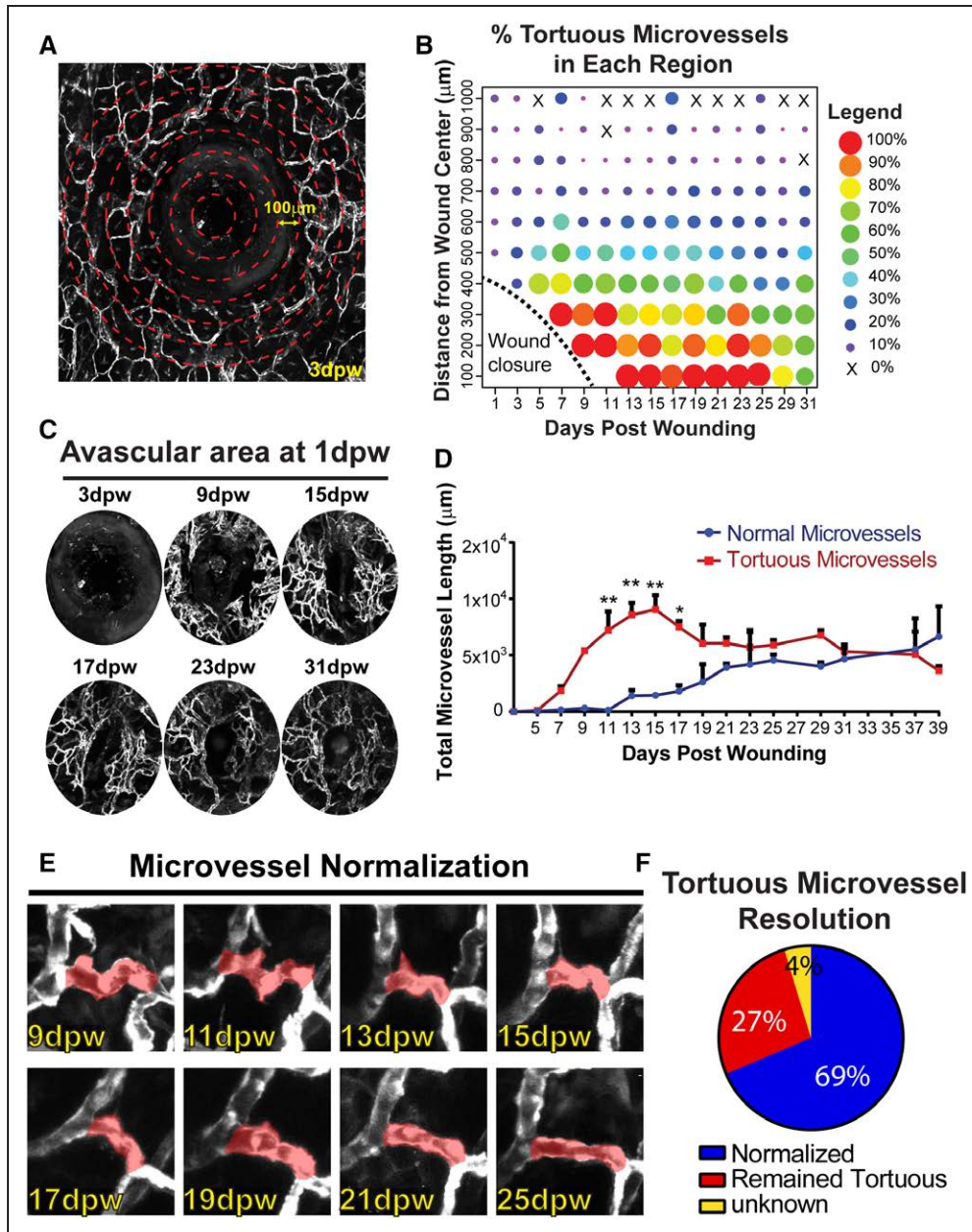


Figure 2. Tortuous microvessel location, formation, and resolution. **A**, Example of 3 dpw wound illustrating defined regions every 100 μm (not to scale). Note avascular area (wound punch+tissue) in segments close to the wound. **B**, Dot plot representing percentage of tortuous microvessels in each region over time. Warmer colors (red/orange), elevated tortuous microvessels; cooler colors (blue/purple), reduced tortuous microvessels. **C**, Avascular wound area+punch, defined at 1 dpw and analyzed at subsequent time points. **D**, Quantification of normal and tortuous microvessel length in new wound tissue (same areas measured for all time points). Error bars, mean+SEM. Statistical comparisons, 2-way ANOVA with Sidak multiple comparisons test. * $P\leq 0.05$, ** $P\leq 0.005$. **E**, Example of a tortuous microvessel over time, showing normalization. **F**, Percentage of vessels that normalized, remained tortuous, or outcome unknown during 39 day wound healing time course. $n=86$ tortuous microvessels. Vessels pseudocolored using Photoshop. ANOVA indicates analysis of variance; and dpw, days post-wounding.

linear capillaries, and microsphere patterns changed completely from one time frame to the next (Figure 3B through 3F, blue boxes). In contrast, some microspheres appeared to stick in the curved area of tortuous microvessels, and these became more prevalent with time (Figure 3B through 3G, red boxes), while the linear regions lost association with microspheres over time as they were presumably cleared from the circulation. Analysis revealed that on average 5 beads per tortuous microvessel remained stationary post-injection, while no beads were stationary in linear microvessels (Figure 3H).

These findings indicate that endothelial cells in tortuous microvessels differ from those in linear regions and suggest that reduced or disturbed blood flow is associated with tortuous microvessels, which could ultimately lead to differences in endothelial cell properties between normal and tortuous microvessels.

Because activated endothelial cells are often round rather than being spindle-shaped and elongated, we hypothesized that endothelial cells in tortuous microvessels had abnormal cell shapes. To test this hypothesis, we generated mosaic mouse lines

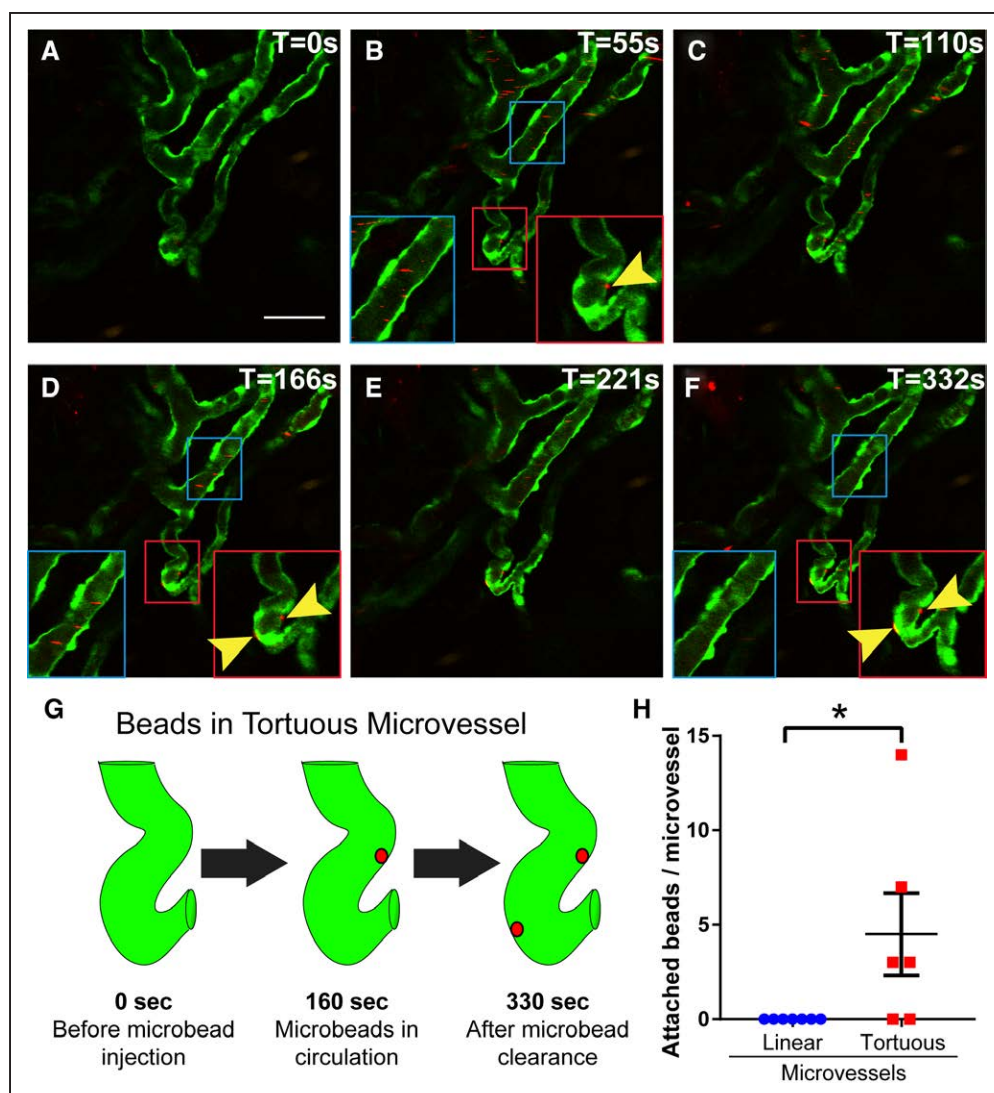


Figure 3. Circulating microspheres accumulate in tortuous microvessels. Representative images from movie of circulating microspheres at 7 dpw; time (T) sec, upper right. **A**, Prior to injection of microspheres into tail vein. **B–F**, Images post-injection at indicated times. Blue insets, linear microvessel; red insets, tortuous microvessel; yellow arrowheads, microspheres stationary for multiple time frames. Note that no microspheres remain in the normal vessel segment (blue inset) as opposed to trapped microspheres in the tortuous microvessel (arrows in red inset). **G**, Illustration showing tortuous microvessel and areas where microspheres became trapped. **H**, Quantification of microsphere trapping in normal and tortuous microvessels; long line and error bars, mean \pm SEM. Statistical comparisons, Student *t* test (unpaired, 2-tailed). * $P < 0.05$. Scale bar, 50 μ m.

that expressed GFP in endothelial cells along with a vascular-selective inducible Cre driver, *Cdh5-CreERT2*,²⁶ and a tdTomato excision reporter.²⁷ The reporter was activated in a small subset of endothelial cells (10%–30%) using low-dose tamoxifen prior to wound healing, and individual groups of endothelial cells were followed during an abbreviated time course (21 days) that, nevertheless, encompassed the major angiogenic period in our model. Endothelial cells in normal capillaries maintained a stereotypical spindle shape, while those in tortuous microvessels were spindle-shaped at 1 dpw, but became more rounded over time, coincident with increased tortuosity (Figure 4A and 4B). The shapes of individual endothelial cells were measured at 11 dpw in fixed samples stained for PECAM-1 (platelet endothelial cell adhesion molecule 1), an endothelial cell border marker (Figure 4C). The longitudinal/transverse axis ratio was significantly reduced in endothelial cells from tortuous microvessels relative to control

endothelial cells in normal microvessels (Figure 4D). These data confirm the visual appearance of endothelial cells in tortuous microvessels as rounded and suggestive of activation.

To determine whether the endothelial cells in tortuous microvessels had other distinct properties, we examined the expression of several markers associated with a proinflammatory phenotype. Expression of ICAM-1 (intercellular adhesion molecule 1), an intercellular adhesion molecule involved in leukocyte extravasation,²⁸ showed robust expression at 15 dpw in tortuous vessels near the wound (Figure IIIA in the [online-only Data Supplement](#)). Likewise, staining for P-selectin, which is associated with postcapillary venules that are competent for extravasation,²⁹ was positive in areas of tortuous microvessels (Figure IIIB in the [online-only Data Supplement](#)).

We next asked whether tortuous vessels had altered barrier function. To test for permeability, we injected smaller

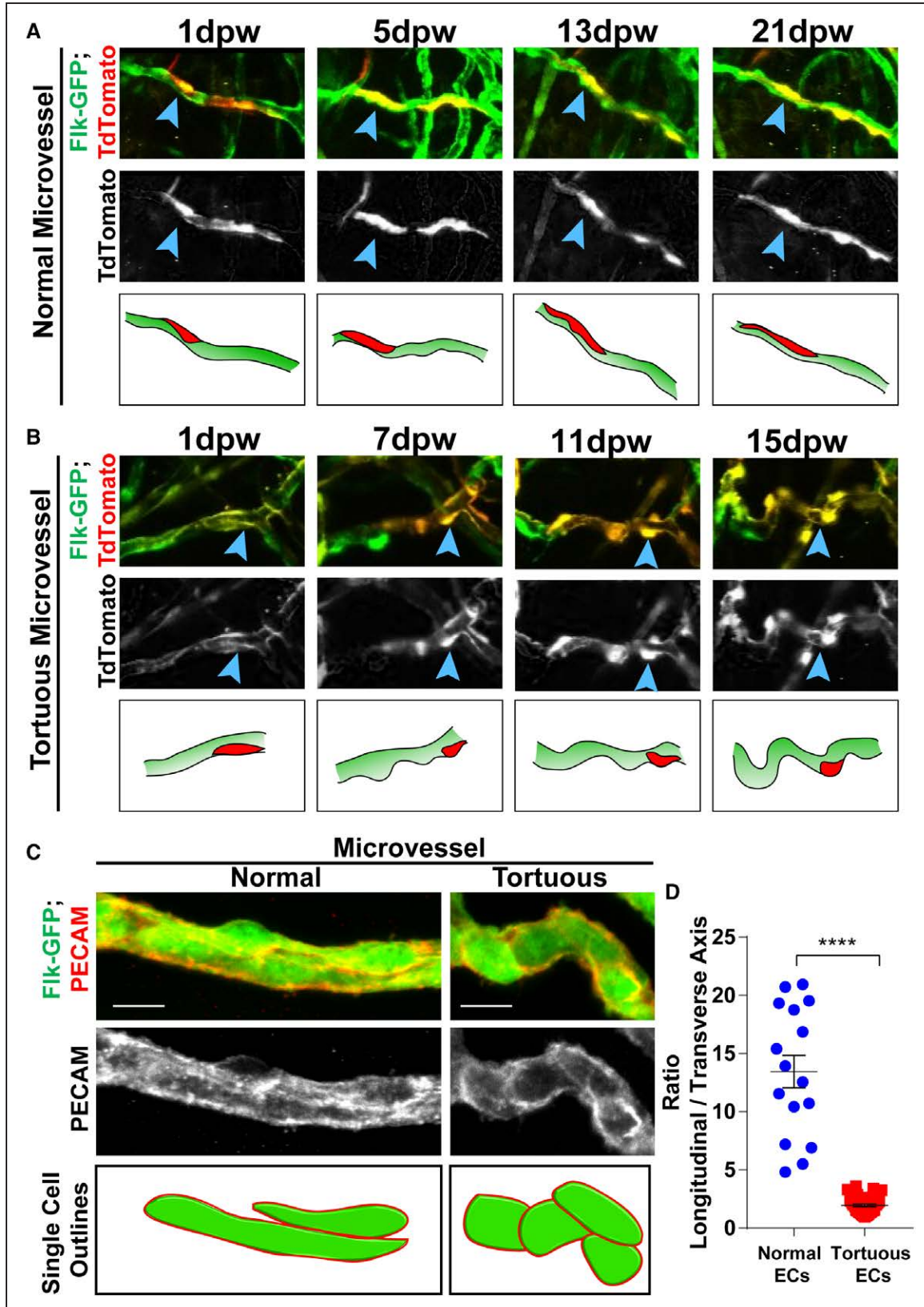


Figure 4. Cellular morphology in tortuous microvessels. Mosaic analysis of microvessels during 21 day wound healing time course in mice of indicated genotype. **A**, Normal microvessel endothelial cell (EC) have stereotypical spindle morphology throughout time course (blue arrow-heads, red cell in diagram). **B**, Tortuous microvessel ECs initiate as spindle-like and become rounded with time and tortuosity (blue arrow-heads, red cell in diagram). **C**, PECAM (platelet endothelial cell adhesion molecule) staining of Fik1-GFP mice at 11 dpw, highlighting individual cell borders. **D**, Ratio of longitudinal to transverse axis of EC in normal and tortuous microvessels; long line and error bars, mean±SEM. Statistical comparisons, Student *t* test (unpaired, 2-tailed); **** $P < 0.0001$. Scale bar, 10 μ m (**C** and **D**). dpw indicates days post-wounding.

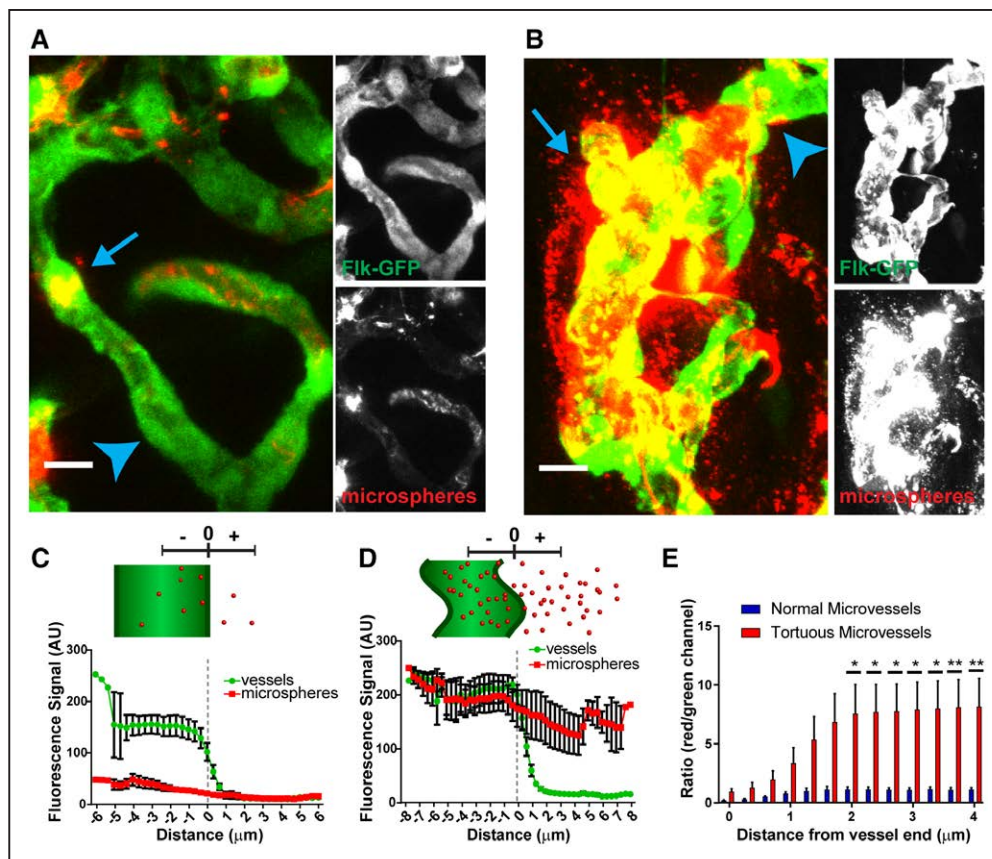


Figure 5. Tortuous microvessels have increased permeability. Analysis of microvessel permeability at 15 dpw. **A** and **B**, Examples of normal (**A**) and tortuous vessel (**B**) images (compressed Z stacks) that were analyzed. **C** and **D**, Top, diagram of vessel and microspheres showing measurements. Bottom, quantification of the fluorescence signal of green and red channels with distance from the center of the vessel, extending outward for one radius length for normal (**C**) and tortuous (**D**) microvessels. **E**, Ratio of microsphere label (red channel) to vessel label (green channel) starting at 0 (edge of vessel). $n=6$ vessel segments in normal vs tortuous microvessels. Long line and error bars, mean \pm SEM. Statistical comparisons, two-way ANOVA with Tukey multiple comparison test; * $P\leq 0.05$; ** $P\leq 0.005$. Scale bar, 10 μm . ANOVA indicates analysis of variance.

fluorescent microsphere beads (20 nm) via tail vein injection at 15 dpw and collected samples after 20 minutes (Figure 5A and 5B). Line scan measurements revealed that microspheres were significantly increased in the areas adjacent to tortuous microvessels relative to normal nearby capillaries (Figure 5C through 5E). Interestingly, we also noted increased microspheres within the tortuous microvessels, consistent with our earlier finding that larger microspheres were enriched in tortuous areas. These results indicate that tortuous vessels have increased permeability, consistent with the cell shape changes. Taken together, these findings show that endothelial cells in tortuous microvessels are distinct from cells in normal capillaries by multiple criteria.

Tortuous Microvessels Sprout Robustly

The altered morphology and properties of tortuous microvessel endothelial cells suggest that they may be more prone to sprouting, than endothelial cells in normal capillaries. Thus, we hypothesized that tortuous microvessel endothelial cells sprout more frequently than normal capillaries, and we used our high-resolution longitudinal data set from the complete time course (39 days) of wound healing to test this idea. Analysis of blood vessel sprouts, defined as new extensions

of at least 10 μm that were unconnected (blind-ended) and that initiated during the wound healing time course, revealed that tortuous microvessels sprouted exuberantly (Figure 6A through 6G). For example, a microvessel near the wound that appeared normal at 1 dpw subsequently became tortuous at 5 dpw, and sprouts emanated from curved regions (Figure 6A and 6B). At 7 dpw, the main microvessel remained tortuous, and the sprouts continued to extend (Figure 6C). By 9 dpw onward, the main microvessel began to normalize, while the sprouts persisted and made connections to each other or to other vessels (Figure 6D through 6F). When analyzing new sprout initiations, we found that tortuous microvessels sprouted at a significantly higher frequency than normal capillaries from 5 to 13 dpw (Figure 6G).

To determine whether sprout initiations from tortuous microvessels were more or less stable than sprout initiations from normal vessels, we quantified how often sprouts from each type of vessel formed a connection or retraction (Figure IVA and IVB in the [online-only Data Supplement](#)). Our analysis showed no significant differences between connections and retractions of sprouts from tortuous or normal microvessels (Figure IVC in the [online-only Data Supplement](#)), suggesting that sprouting from tortuous vessels leads to stable connections and expands the vascular plexus near the wound

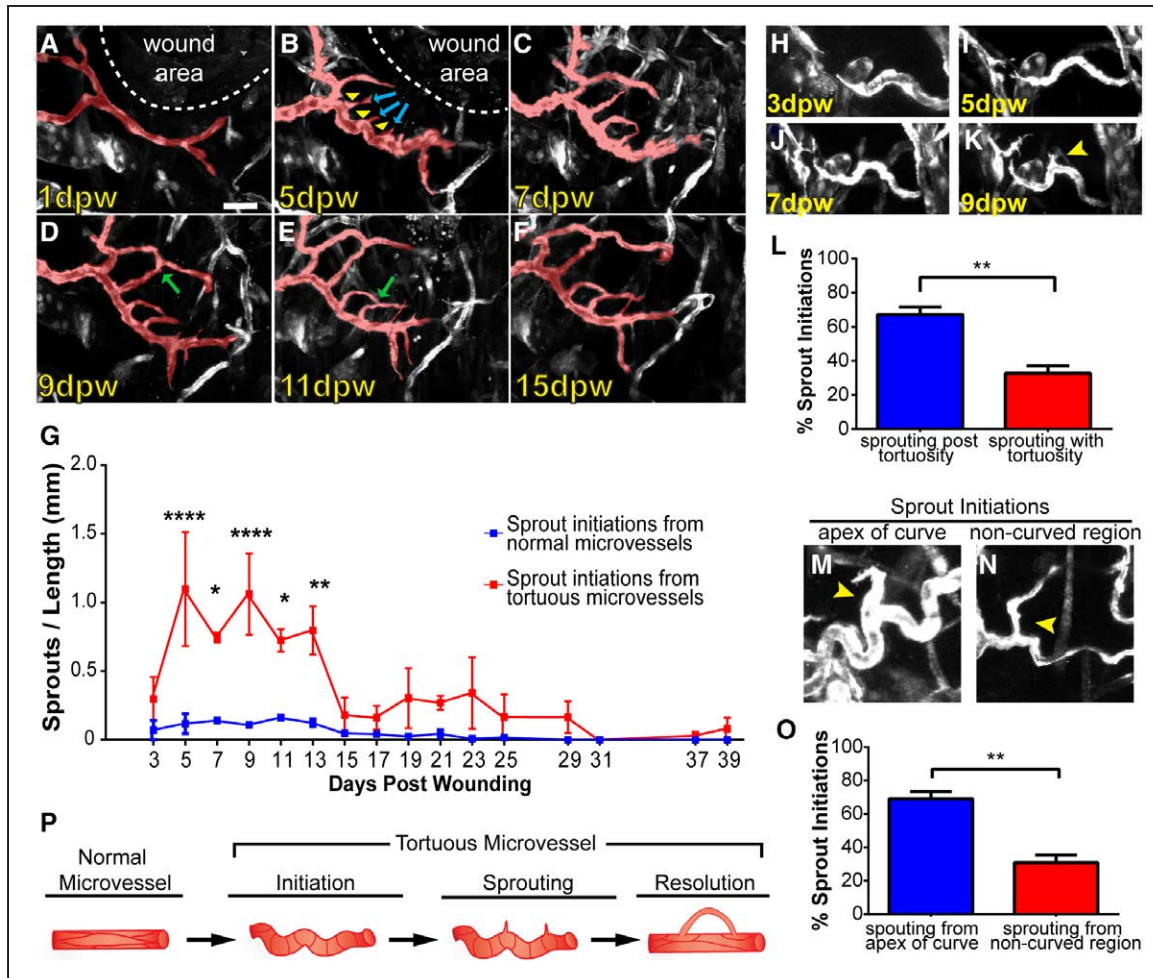


Figure 6. Tortuous microvessels have increased sprouting. Analysis of sprouting from normal and tortuous microvessels over 39 day wound healing time course. **A–F**, Example of a normal microvessel near wound that became tortuous and initiated sprouting. **A**, Normal microvessel near wound at 1 dpw. **B**, At 5 dpw, the main microvessel became tortuous and initiated sprouting (blue arrows) from the apex of curved regions (yellow arrowheads). **C**, Main microvessel remained tortuous and sprouts persisted at 7 dpw. **D–F**, From 9 to 15 dpw, the main tortuous microvessel was normalized, and the sprouts formed new connections (green arrows). **G**, Quantification of sprout initiations from normal and tortuous microvessels during wound healing, $n=3$ ears. Error bars, mean \pm SEM; Statistical comparisons: 2-way ANOVA with Sidak multiple comparisons test. * $P\leq 0.05$; ** $P\leq 0.005$; **** $P\leq 0.0005$. **H–K**, Example of sprout initiation after tortuous microvessel formation. Note that sprout initiation does not occur until 9 dpw (**K**, yellow arrow). **L**, Quantification of sprout initiations subsequent to tortuous microvessel formation relative to sprout initiations simultaneous with tortuous microvessel formation. Error bars, mean \pm SEM; Statistical comparisons: Student t test (unpaired, 2-tailed); ** $P\leq 0.005$. **M**, Example of sprout initiation from apex of curve on tortuous microvessel. **N**, Example of sprout initiation from noncurved region of tortuous microvessel. **O**, Quantification of sprout initiations from the apex of tortuous microvessels relative to noncurved regions. Error bars, mean \pm SEM; Statistical comparisons: Student t test (unpaired, 2-tailed); ** $P\leq 0.005$. **P**, Model of tortuous microvessel initiation, sprouting, and resolution during wound healing. Scale bar, 50 μ m (**A**). Vessels pseudocolored using Photoshop. dpw indicates days post-wounding.

site. We asked whether sprouting from tortuous microvessels was a resolution mechanism and found that 36% of tortuous microvessels normalized after sprouting, while 54% normalized without sprouting, suggesting that sprouting is not required for vessel normalization (Figure IVD in the [online-only Data Supplement](#)).

To better understand the sprouting behavior of tortuous microvessels, we examined when sprout initiations occurred relative to acquisition of microvessel tortuosity (Figure 6H through 6L). This analysis showed that significantly more sprouts formed after microvessels became tortuous compared with sprouts initiating coincident with tortuosity (Figure 6L), indicating that sprouting is downstream of tortuous vessel formation. This data suggest that tortuous vessel formation

promotes endothelial cell sprouting. To determine whether some regions within tortuous microvessels were more prone to sprouting, we measured sprout initiations from curved regions versus noncurved regions of tortuous microvessels. Our data revealed a significant increase in sprout frequency from the apex of the curved region of tortuous microvessels versus other areas of the vessel (Figure 6M through 6O), suggesting that these curved areas are the most sprout-prone regions of tortuous microvessels. Taken together, these data support our hypothesis that endothelial cells in tortuous microvessels are distinct, and the enhanced sprouting frequency combined with enhanced overall tortuosity suggest that tortuous microvessel formation is a key player during the angiogenic phase of wound healing.

Discussion

Here, we identify tortuous microvessels for the first time and present a longitudinal, in-depth analysis of microvessel tortuosity during wound healing. Microvessel tortuosity increases over a reproducible time course that largely correlates with increased overall angiogenesis. We show that sprouting is promoted from tortuous microvessels, and this exuberant sprouting likely contributes significantly to wound angiogenesis and overall healing. Our data are consistent with a model whereby tortuosity alters flow parameters and leads to endothelial cell activation that promotes sprouting in these regions (Figure 6P). Thus, the emergence of tortuous microvessels near a wound site may be a mechanism to efficiently expand wound angiogenesis and promote healing.

Although tortuous vessels have been observed during wound healing and in diseases such as cancer,^{16,30} microvessels of the caliber (5–20 μm) analyzed here were not resolved by most of these studies. Yet the bulk of the vasculature in most vessel beds comprised small-caliber capillaries, and these capillaries are usually the source of sprouts that contribute to neoangiogenesis. While some studies analyzed static images of wound vessels,^{16,31,32} our approach allowed for high spatiotemporal resolution of microvessels and longitudinal analysis of this critical component of wound healing. Our finding that tortuous microvessels contribute significantly to overall sprouting angiogenesis in the wound environment, and our results showing that these sprouts often lead to new connections and conduits, provide a novel link between vessel tortuosity and wound healing via sprouting angiogenesis.

Sprouting from tortuous microvessels occurs at a higher frequency than from normal vessels, and these sprouts often initiate from the apex of curved regions of tortuous microvessels. While we do not have the resolution to interrogate junctional integrity, our finding that tortuous microvessels are leakier than normal capillaries, and that microspheres become stuck in the tortuous microvessels, suggests altered blood flow and shear stress. Interestingly, a recent study by Ghaffari et al³³ showed that sprouts emanate from the lowest minimum in predicted shear stress along a capillary network, indicating that reduced shear stress promotes sprouting events. Given these results, and our live capture of circulating microspheres, we predict that shear stress is lower and disturbed in tortuous microvessels relative to normal capillaries downstream of altered vessel morphology. The altered shape of endothelial cells within tortuous microvessels is consistent with this idea because relative loss of the laminar flow vector is predicted to loosen junctions and promote sprouting. Likewise, the enhanced sprout initiations we observed from the apex of curved regions suggest that altered flow may induce local discontinuities that are optimized for sprouting in those regions.

What triggers tortuous microvessel formation during wound healing? It is likely a complex combination of local environmental cues and other changes associated with wound healing because the tortuous microvessels resolve over time. The peak frequency of tortuous microvessels roughly corresponds to the angiogenic phase of wound healing,¹⁷ and it is known that proangiogenic cytokines such as VEGF (vascular endothelial growth factor) induce tortuosity.^{18,30,34} Although

the highest window of VEGF expression in the wound occurs from 3 to 7 days post-wounding, it is likely that other proangiogenic growth factors, such as bFGF (basic fibroblast growth factor), contribute to tortuous vessel formation at later stages.³⁵ Tortuous microvessels are enriched close to the wound border, which is the most hypoxic area of the wound, consistent with proangiogenic influences. However, proangiogenic signals are not sufficient to induce vessel tortuosity because most developmental angiogenesis occurs independent of tortuosity. Wound healing is also associated with transient inflammation, so proinflammatory cytokines may also contribute to microvessel tortuosity. Additionally, cytoskeletal rearrangements accompany endothelial cell shape changes and sprouting migration,³⁶ and growth factors induce cytoskeletal changes,^{37,38} so the elevated growth factors found in the wound healing environment likely contribute in complex ways to microvessel tortuosity. In any case, it is likely that local changes in the wound healing environment promote tortuosity, and this work shows that vessel tortuosity contributes substantially to microvessel sprouting and neoangiogenesis that promotes wound healing.

In tumor microenvironments, microvessels readily become tortuous,^{23,34} which may decrease antitumor drug efficacy.¹¹ The wound healing process is a natural physiological response, but wound healing is compromised in some diseases as a result of defective vascularization. For example, wound healing is often defective in diabetic patients and sometimes results in limb amputation, and a defective angiogenic response from the microcirculation contributes to this dysfunction.^{39,40} Furthermore, with time and increasing vessel dysfunction, tortuosity subsides in larger vessels of diabetic patients but increases in capillary-sized vessels.³¹ The microcirculation comprises capillaries that make up the bulk of the vasculature and readily respond to signaling cues. Here, we identify a new class of vessel, a tortuous microvessel, that is associated with wound healing and contributes significant angiogenic sprouting to the process. Knowledge of the contribution of tortuous microvessels to angiogenic sprouting and wound healing will be useful in designing new therapeutic approaches to accelerate and improve wound healing.

Acknowledgments

We thank Bautch lab members for productive discussions and input, Robert Curran of the University of North Carolina (UNC) Hooker Imaging Core for technical support on the FV1000MPE, and the UNC Animal Studies Core for support.

Sources of Funding

This work was supported by grants to V.L. Bautch (National Institutes of Health [NIH] HL43174, HL116719) and fellowship support to D.C. Chong (National Science Foundation DGE-1144081; American Heart Association [AHA] 15PRE25090082; NIH 5F31HL129762).

Disclosures

None.

References

1. Adams RH, Alitalo K. Molecular regulation of angiogenesis and lymphangiogenesis. *Nat Rev Mol Cell Biol.* 2007;8:464–478. doi: 10.1038/nrm2183.

2. Chappell JC, Wiley DM, Bautch VL. How blood vessel networks are made and measured. *Cells Tissues Organs*. 2012;195:94–107. doi: 10.1159/000331398.
3. Herbert SP, Stainier DY. Molecular control of endothelial cell behaviour during blood vessel morphogenesis. *Nat Rev Mol Cell Biol*. 2011;12:551–564. doi: 10.1038/nrm3176.
4. Folkman J. Angiogenesis. *Annu Rev Med*. 2006;57:1–18. doi: 10.1146/annurev.med.57.121304.131306.
5. Risau W. Mechanisms of angiogenesis. *Nature*. 1997;386:671–674. doi: 10.1038/386671a0.
6. Chung AS, Ferrara N. Developmental and pathological angiogenesis. *Annu Rev Cell Dev Biol*. 2011;27:563–584. doi: 10.1146/annurev-cellbio-092910-154002.
7. Kushner EJ, Bautch VL. Building blood vessels in development and disease. *Curr Opin Hematol*. 2013;20:231–236. doi: 10.1097/MOH.0b013e328360614b.
8. Dvorak HF. Tumors: wounds that do not heal-redux. *Cancer Immunol Res*. 2015;3:1–11. doi: 10.1158/2326-6066.CIR-14-0209.
9. Nagy JA, Chang SH, Dvorak AM, Dvorak HF. Why are tumour blood vessels abnormal and why is it important to know? *Br J Cancer*. 2009;100:865–869. doi: 10.1038/sj.bjc.6604929.
10. Helisch A, Schaper W. Arteriogenesis: the development and growth of collateral arteries. *Microcirculation*. 2003;10:83–97. doi: 10.1038/sj.mn.7800173.
11. Jain RK. Normalizing tumor vasculature with anti-angiogenic therapy: a new paradigm for combination therapy. *Nat Med*. 2001;7:987–989. doi: 10.1038/nm0901-987.
12. Taarnhøj NC, Munch IC, Sander B, Kessel L, Hougaard JL, Kyvik K, Sørensen TI, Larsen M. Straight versus tortuous retinal arteries in relation to blood pressure and genetics. *Br J Ophthalmol*. 2008;92:1055–1060. doi: 10.1136/bjo.2007.134593.
13. Rege A, Thakor NV, Rhie K, Pathak AP. *In vivo* laser speckle imaging reveals microvascular remodeling and hemodynamic changes during wound healing angiogenesis. *Angiogenesis*. 2012;15:87–98. doi: 10.1007/s10456-011-9245-x.
14. Pijnenborg R, Vercruyse L, Hanssens M. The uterine spiral arteries in human pregnancy: facts and controversies. *Placenta*. 2006;27:939–958. doi: 10.1016/j.placenta.2005.12.006.
15. Schaper W, Buschmann I. Arteriogenesis, the good and bad of it. *Cardiovasc Res*. 1999;43:835–837.
16. Han HC. Twisted blood vessels: symptoms, etiology and biomechanical mechanisms. *J Vasc Res*. 2012;49:185–197. doi: 10.1159/000335123.
17. Greaves NS, Ashcroft KJ, Baguneid M, Bayat A. Current understanding of molecular and cellular mechanisms in fibroplasia and angiogenesis during acute wound healing. *J Dermatol Sci*. 2013;72:206–217. doi: 10.1016/j.jdermsci.2013.07.008.
18. Wong VW, Crawford JD. Vasculogenic cytokines in wound healing. *Biomed Res Int*. 2013;2013:190486. doi: 10.1155/2013/190486.
19. Singer AJ, Clark RA. Cutaneous wound healing. *N Engl J Med*. 1999;341:738–746. doi: 10.1056/NEJM199909023411006.
20. Hashizume H, Baluk P, Morikawa S, McLean JW, Thurston G, Roberge S, Jain RK, McDonald DM. Openings between defective endothelial cells explain tumor vessel leakiness. *Am J Pathol*. 2000;156:1363–1380. doi: 10.1016/S0002-9440(10)65006-7.
21. Jung Y, Dziennis S, Zhi Z, Reif R, Zheng Y, Wang RK. Tracking dynamic microvascular changes during healing after complete biopsy punch on the mouse pinna using optical microangiography. *PLoS One*. 2013;8:e57976. doi: 10.1371/journal.pone.0057976.
22. Manning CS, Jenkins R, Hooper S, Gerhardt H, Marais R, Adams S, Adams RH, van Rheenen J, Sahai E. Intravital imaging reveals conversion between distinct tumor vascular morphologies and localized vascular response to Sunitinib. *IntraVital*. 2013;2:e24790. doi: 10.4161/intv.24790.
23. Pitynski K, Litwin JA, Richter P, Miodonski AJ. Microvascular architecture of human epicolic and paracolic lymph nodes located in the vicinity of colon cancer: a SEM study of corrosion casts. *Pathol Res Pract*. 2012;208:94–99. doi: 10.1016/j.prp.2011.12.008.
24. Ema M, Takahashi S, Rossant J. Deletion of the selection cassette, but not cis-acting elements, in targeted Flk1-lacZ allele reveals Flk1 expression in multipotent mesodermal progenitors. *Blood*. 2006;107:111–117. doi: 10.1182/blood-2005-05-1970.
25. Kerber CW, Liepsch D. Flow dynamics for radiologists. II. Practical considerations in the live human. *AJNR Am J Neuroradiol*. 1994;15:1076–1086.
26. Sørensen I, Adams RH, Gossler A. DLL1-mediated Notch activation regulates endothelial identity in mouse fetal arteries. *Blood*. 2009;113:5680–5688. doi: 10.1182/blood-2008-08-174508.
27. Madisen L, Zwingman TA, Sunkin SM, Oh SW, Zariwala HA, Gu H, Ng LL, Palmiter RD, Hawrylycz MJ, Jones AR, Lein ES, Zeng H. A robust and high-throughput Cre reporting and characterization system for the whole mouse brain. *Nat Neurosci*. 2010;13:133–140. doi: 10.1038/nn.2467.
28. Lawson C, Wolf S. ICAM-1 signaling in endothelial cells. *Pharmacol Rep*. 2009;61:22–32.
29. Fuxe J, Lashnits E, O'Brien S, Baluk P, Tabruyn SP, Kuhnert F, Kuo C, Thurston G, McDonald DM. Angiopoietin/Tie2 signaling transforms capillaries into venules primed for leukocyte trafficking in airway inflammation. *Am J Pathol*. 2010;176:2009–2018. doi: 10.2353/ajpath.2010.090976.
30. Saaristo A, Veikkola T, Enhölm B, Hytönen M, Arola J, Pajusola K, Turunen P, Jeltsch M, Karkkainen MJ, Kerjaschki D, Bueler H, Ylä-Herttua S, Alitalo K. Adenoviral VEGF-C overexpression induces blood vessel enlargement, tortuosity, and leakiness but no sprouting angiogenesis in the skin or mucous membranes. *FASEB J*. 2002;16:1041–1049. doi: 10.1096/fj.01-1042com.
31. Owen CG, Newsom RS, Rudnicka AR, Barman SA, Woodward EG, Ellis TJ. Diabetes and the tortuosity of vessels of the bulbar conjunctiva. *Ophthalmology*. 2008;115:e27–e32. doi: 10.1016/j.ophtha.2008.02.009.
32. Kim KE, Cho CH, Kim HZ, Baluk P, McDonald DM, Koh GY. *In vivo* actions of angiopoietins on quiescent and remodeling blood and lymphatic vessels in mouse airways and skin. *Arterioscler Thromb Vasc Biol*. 2007;27:564–570. doi: 10.1161/01.ATV.0000256458.82320.be.
33. Ghaffari S, Leask RL, Jones EA. Flow dynamics control the location of sprouting and direct elongation during developmental angiogenesis. *Development*. 2015;142:4151–4157. doi: 10.1242/dev.128058.
34. Lee S, Jilani SM, Nikolova GV, Carpizo D, Iruela-Arispe ML. Processing of VEGF-A by matrix metalloproteinases regulates bioavailability and vascular patterning in tumors. *J Cell Biol*. 2005;169:681–691. doi: 10.1083/jcb.200409115.
35. Bao P, Kodra A, Tomic-Canic M, Golinko MS, Ehrlich HP, Brem H. The role of vascular endothelial growth factor in wound healing. *J Surg Res*. 2009;153:347–358. doi: 10.1016/j.jss.2008.04.023.
36. Kopecki Z, Cowin AJ. The role of actin remodelling proteins in wound healing and tissue regeneration. In: V. A. Alexandrescu, ed. *Wound Healing—New Insights Into Ancient Challenges*. Rijeka: InTech; 2016: Ch. 06.
37. Morales-Ruiz M, Fulton D, Sowa G, Languino LR, Fujio Y, Walsh K, Sessa WC. Vascular endothelial growth factor-stimulated actin reorganization and migration of endothelial cells is regulated via the serine/threonine kinase Akt. *Circ Res*. 2000;86:892–896.
38. Dethlefsen SM, Butterfield CE, Ausprunk DH. Structural changes induced in capillary endothelial cells by growth factors: altered distribution of cytoskeletal elements and organelles in cells spreading in the presence of tumor conditioned medium and hypothalamus derived growth factor. *Tissue Cell*. 1986;18:827–837.
39. Brem H, Tomic-Canic M. Cellular and molecular basis of wound healing in diabetes. *J Clin Invest*. 2007;117:1219–1222. doi: 10.1172/JCI32169.
40. Taherogorabi Z, Khazaei M. Imbalance of angiogenesis in diabetic complications: the mechanisms. *Int J Prev Med*. 2012;3:827–838.

Highlights

- We identify a new type of transient wound-associated vessel called tortuous microvessels.
- Endothelial cells in tortuous microvessels have properties that promote sprouting.
- Tortuous microvessels sprout exuberantly and contribute significantly to wound neoangiogenesis.